Modeling Dot Gain and Inks Interaction

Silvia Zuffi° and Raimondo Schettini[§]
°ITC, Consiglio Nazionale delle Ricerche
[§]DISCO, Università degli Studi di Milano Bicocca
Milano, Italy

Abstract

Multispectral printer characterization requires an effective model to map printer input digital counts into reflectance spectra and vice versa. This paper presents a novel strategy to describe dot gain and interaction among inks in the definition of a printer model employing the Yule Nielsen Spectral Neugebauer equation. The method proposed, that requires the printing and measuring of a training set of 143 colors, has been designed for a four-ink inkjet printer, but its formulation is general and may therefore be extended to be used for characterizing devices having more than four inks. To test the feasibility of the our printer model, we employed an Epson Stylus Color 740 inkjet printer: on a data set consisting of 777 samples, regularly distributed in the HSV color space, we have obtained an average spectral accuracy, in terms of mean root mean squared error, of 0.59% and an average color error of 1.54 ΔE^{*}_{ab}.

Introduction

In the recent years, multispectral reproduction is attracting increasing attention triggered by its appealing feature of significantly reducing undesirable metamerism effects with respect to traditional colorimetric approaches.[1] In multispectral reproduction the aim is to produce, in print, a color having reflectance equal to that of the input color, specified throughout a reflectance spectrum. Multispectral reproduction requires spectral-based printer characterization, that is the definition of a procedure to map printer input digital counts into reflectance spectra and vice versa. Techniques for spectral-based printer characterization commonly employ analytical models, formulated on the basis of the physics behind the printing process. In the modeling of binary printers, most of the methods are based on the color-mixing model of Neugebauer.[2-4] The model, in its original formulation, predicts the outcome of a print with poor accuracy, and several strategies for its upgrading have been proposed. The Yule-Nielsen coefficient, introduced to take into account the effects of light scattering in the substrate, increases the model's performance, but the resulting Yule-Nielsen Spectral Neugebauer model still needs solutions to deal with interactions among inks and of inks with paper. More complex methods have been introduced to describe optical dot gain, among which the convolution with a point spread function (PSF),[5] or probability models.[6,7] Alternative approaches describe the spreading of the ink by enlarging the drop impact on the basis of the configuration of its neighbors and the state of the surface,[8,9] or by modeling the physical dot gain with a transmission function defined on a blurred version of the halftone image.[5] Other methods for the improvement of model accuracy employ cellular approaches[10] or ascribe partial uncertainty to the measurements of reflectance. Examples of methods that take this circumstance into account are Refs. 11 and 12. In this work, we present a novel method to describe dot gain and inks interaction in the context of the use of the Yule-Nielsen Spectral Neugebauer model for spectral-based printer characterization.

The Neugebauer Printer Model

According to the Yule-Nielsen Spectral Neugebauer (YNSN) equation, the spectrum of an N-inks halftone print is the weighted sum of 2^N different colors, called Neugebauer primaries, given by all the possible overprints of inks. The weight of each Neugebauer primary is the area it covers in the halftone cell. The YNSN model for a 4-ink halftone print is:

$$R_{pr\,int,\lambda} = \left[\sum_{p=0}^{15} a_p R_{p,\lambda}^{\frac{1}{n}} \right]^n \qquad \lambda = 1..\Gamma \qquad (1)$$

where $R_{print,\lambda}$ is the reflectance of the printed color, n is the Yule-Nielsen factor, $R_{p,\lambda}$ is the reflectance of the p-th Neugebauer primary, a_p is the primary area coverage, and reflectance are vectors of Γ real numbers in the range [0, 1] corresponding to a sampling of the visible range of wavelengths. The area coverage is the percentage of the halftone cell covered by the Neugebauer primary.

The computation of area coverage depends on the dots placement on the substrate. The Demichel model can be used to compute the percentage of the area covered by each primary if the placement is statistically independent; if this is the case, the dot overlap is the product of the relative area covered by single inks. This model is considered valid for random or rotated halftone screen;[13] it fails in all cases in which there is a singular screen superposition, although the color deviation observed is not excessively large.[14] For dot-on-dot printing a different formulation must be considered.[15] According to the Demichel model, area coverage is computed with equations in Table 1.

Table 1. The calculus of the area coverage from effective concentrations of inks. The dependence from theoretical concentration has been omitted for simplicity.

INDEX, P	N. PRIMARY	AREA COVERAGE, a_p
1	K	$(1-c_{ck})\,(1-m_{mk})\,(1-y_{yk})\,k_k$
2	Y	$(1-c_{cy})\,(1-m_{my})\,y_y\,(1-k_{yk})$
3	YK	$(1-c_{cyk})\,(1-m_{myk})\,y_{yk}\,k_{yk}$
4	M	$(1-c_{cm})\,m_m\,(1-y_{my})\,(1-k_{mk})$
5	MK	$(1-c_{cmk})\,m_{mk}\,(1-y_{myk})\,k_{mk}$
6	R	$(1-c_{cmy})\,m_{my}\,y_{my}\,(1-k_{myk})$
7	RK	$(1-c_{cmyk})\,m_{myk}\,y_{myk}\,k_{myk}$
8	C	$c_c\,(1-m_{cm})\,(1-y_{cy})\,(1-k_{ck})$
9	CK	$c_{ck}\,(1-m_{cmk})\,(1-y_{cyk})\,k_{ck}$
10	G	$c_{cy}\,(1-m_{cmy})\,y_{cy}\,(1-k_{cyk})$
11	GK	$c_{cyk}\,(1-m_{cmyk})\,y_{cyk}\,k_{cyk}$
12	B	$c_{cm}\,m_{cm}\,(1-y_{cmy})\,(1-k_{cmk})$
13	BK	$c_{cmk}\,m_{cmk}\,(1-y_{cmyk})\,k_{cmk}$
14	CMY	$c_{cmy}\,m_{cmy}\,y_{cmy}\,(1-k_{cmyk})$
15	CMYK	$c_{cmyk}\,m_{cmyk}\,y_{cmyk}\,k_{cmyk}$

Modeling Dot Gain and Ink Interaction

The inaccuracy of the YNSN model is ascribable to the nonlinear relationship, due to the combination of optical and mechanical dot gain, between the theoretical concentration of the ink on paper and its effective concentration. In practice, inaccuracy may come from measurement errors, and partial uncertainty may be therefore assumed on Neugebauer primaries reflectance.[11,12] In our approach, we consider that the inaccuracy of the YNSN model derives only from errors in the inks area coverage prediction. An example of the dot growth effect is indicated in Figure 1. Theoretical concentration corresponds to the percentage of requested ink, as indicated from the digital counts sent to the printer, and effective concentration is the percentage of area the dot actually covers in the halftone cell. In the following, this relationship is called *dot gain function*, and, in general, peaks at around 50% of the theoretical concentration.

Dot gain functions are commonly used to model the spread of inks on paper, but the spread may be altered when covering previously deposited ink. Various strategies have been suggested to account for this phenomenon.[16,3]

In this work, we propose to account for the interaction among inks by providing a different dot gain function for any overprint. Table 1 specifies the dot gain functions that have to be considered to compute the area coverage of each Neugebauer primary in Equation 1.

For example, if $\mathbf{c} = [c_t, m_t, y_t, k_t]$ is the vector of theoretical concentrations of inks for a given color, according to Table 1, the area coverage of the Neugebauer primary C (cyan) is:

$$a_8 = c_c(c_t)(1 - m_{mc}(m_t))(1 - y_{yc}(y_t))(1 - k_{kc}(k_t)).$$
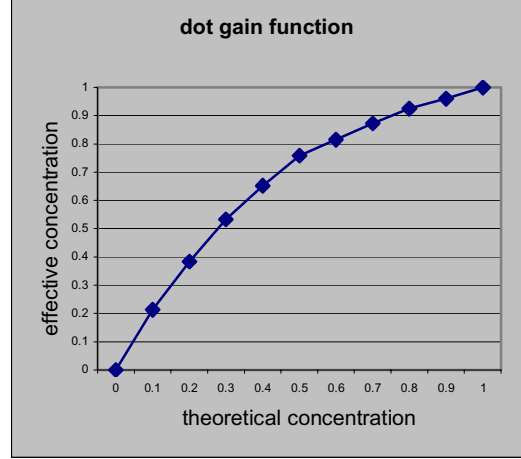
a)
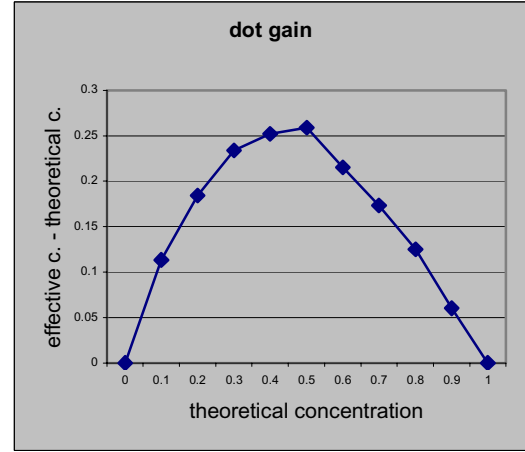
b)

Figure 1. a) Plot of the effective concentration of ink against theoretical concentration. The plot has been obtained by computing the effective concentration as

$$c = 1/\Gamma \sum_{\lambda}[(R_{\lambda} - R_{paper,\lambda})/(R_{ink,\lambda} - R_{paper,\lambda})],$$

for a ramp of eleven cyan color patches printed with an Epson Stylus Color 740, corresponding to theoretical concentrations regularly distributed in the range [0, 1]. b) Plot of the dot gain of ink against theoretical concentration. Dot gain is computed as difference between the effective and the theoretical concentrations in a).

The subscripts in each dot gain function indicate the function to be used; for the cyan ink the model lists 8 different dot gain functions, which depend on the inks in the Neugebauer primary. For example, in Table 1, c_{cy} is the dot gain function of cyan when computing the area coverage of the Neugebauer primary G (green, the overprint of cyan and yellow), as $a_{10} = c_{cy}(c_t)(1 - m_{cmy}(m_t))y_{cy}(y_t)(1 - k_{cyk}(k_t))$. The same dot gain function, c_{cy}, is used to compute the effective concentration of cyan in the Neugebauer primary Y (yellow).

And, in area coverage of G, the dot gain of magenta, m_{cmy} refers to the presence of cyan and yellow. Moreover it refers to the presence of magenta, otherwise its effective concentration would be zero. The area of paper coverage is computed as the difference between the sum of the area coverage of the inks and their overprints, with the constraint to be positive:

$$a_0 = 1 - \sum_{p=1}^{15} a_p, \quad a_0 \geq 0 \qquad (2)$$

In our strategy, we represent the dot gain of an ink in presence of another ink as a variation of the dot gain of ink on paper.

$$ink_{ink,ink2}(ink_t) = ink_{ink}(ink_t) + \Delta ink_{ink2}(ink_t) \qquad (3)$$

where ink_t is the theoretical concentration, one of $\mathbf{c} = [c_t, m_t, y_t, k_t]$.

If we consider, as example, a color produced by the cyan ink and black, the dot gain of cyan in the presence of black ink, c_{ck}, is expressed by the dot gain of cyan on paper, c_c, plus a term c_k, and similarly for black:

$$c_{ck}(c_t) = c_c(c_t) + \Delta c_k(c_t)$$
$$k_{ck}(k_t) = k_k(k_t) + \Delta k_c(k_t) \qquad (4)$$

The dot gain function of a single ink on paper is represented with a cubic spline function composed by 11 knots. The variations of the single-ink dot gain function to account for inks interaction are modeled as follows:

$$\Delta ink = A \exp\left(-\frac{(ink_t - \mu)^2}{s}\right) ink_t (1 - ink_t) \qquad (5)$$

where ink_t is the theoretical concentration, one of $\mathbf{c} = [c, m, y, k]$, A, μ and s are model's parameters. Plots describing the model for different values of parameters are reported in Figure 2.

The proposed model considers the alteration of dot gain dependent only on the ink's theoretical concentration: in case of multi-layer overprints, the presence of other inks is accounted, as a mean effect, by function parameters that are specific for the type of inks, but independent from their concentrations. It is worth noting that the same approach has been adopted by Tzeng,[17] as a solution to achieve better accuracy respect with previously proposals that considered the concentrations of secondary inks.[3]

a)

b)

c)
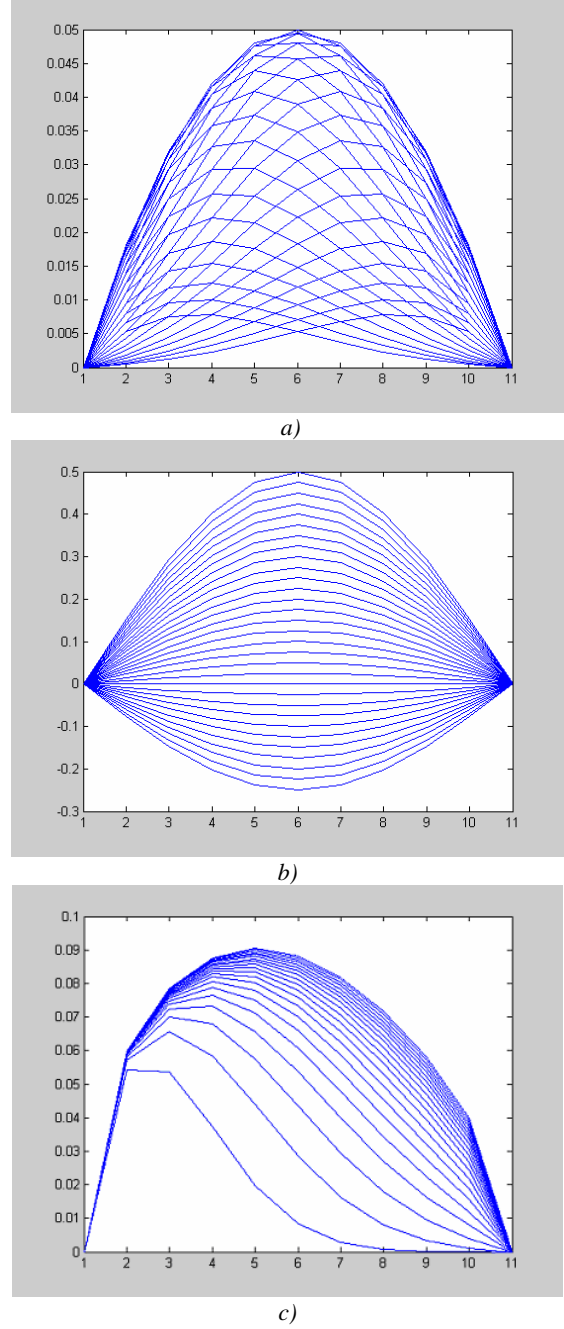
Figure 2. Ink variation model (Equation (5)) for different values of A (a), μ (b) and s (c).

The optical dot gain, theoretically modeled by the Yule-Nielsen coefficient, clearly depends on the characteristics of the substrate and ink layers. Values of n may have a physical meaning for $n < 2$, but, as observed by Viggiano,[18] the fringe in the shape of inks dots causes an increase of n, which may overcome the theoretical limit of 2. In practice, the Yule-Nielsen coefficient is allowed to assume the value that minimizes the accuracy error of the model and is treated as an optimization parameter. To improve the model fit, it can

also be allowed to vary with wavelength.[19] This approach has been followed in our work, while dot gain functions have been considered wavelength-independent. Increasing the value of *n* brings to a reduction in the spectral match error if none dot gain function is employed to describe effective concentrations. We consider the optimum *n* as the value that better reduces the wavelength-dependence in the effective concentration. In practice, we assume that the optimization of the wavelength-dependent *n-value* accounts for optical dot gain, being presumably the light scattering related to wavelength.[2] The mechanical dot gain, modeled by dot gain functions, is instead considered wavelength-independent. The *n-value* and dot gain functions optimization must therefore be performed simultaneously. The tunable parameters in the dot gain functions and the values of the Yule Nielsen coefficient, for each wavelength, are estimated by a model fit optimization phase employing genetic algorithms. The cost function to minimize is:

$$fitness = \frac{1}{S} \cdot \left(\sum_{s=1}^{S} \frac{1}{\Gamma} \cdot \left(\sum_{\lambda=1}^{\Gamma} (R_{print,\lambda,s} - R_{meas,\lambda,s})^2 \right) \right) \quad (6)$$

where S is the number of samples in the training set, Γ is the number of wavelength samples, R_{print} is the reflectance computed with the YNSN model (Equation (1)) and R_{meas} is the measured reflectance of the training set.

Experiment

To test the feasibility of the proposed model, we employed an Epson Stylus Color 740 inkjet printer. The training set is composed by ramps of eleven patches, ranging from the absence of ink to full ink coverage of cyan, magenta, yellow, red, green, blue, black, cyan with black, magenta with black, yellow with black, red with black, green with black and blue with black. The training set is composed of 143 samples. The Neugebauer primaries are obtained by measuring the printed inks at full coverage, and their overprints, by successive prints on the same sheet (Figure 3).

The test set consists of 777 samples, regularly distributed in the HSV color space. Measurements of the spectra are executed with a Gretag Spectrolino, considering values in the wavelength range from 400 to 700 nm with a step of 10 nm. In Figure 4, a graphical representation of the model is reported. Input theoretical concentration are computed from test set RGB data.

The results are reported in terms of color difference in CIELAB ΔE^*_{ab} and root mean square error in Table 2. Plots of the worst test set result, according to the RMS error and CIELAB ΔE^*_{ab} error are reported in Figure 5 and Figure 6, respectively.
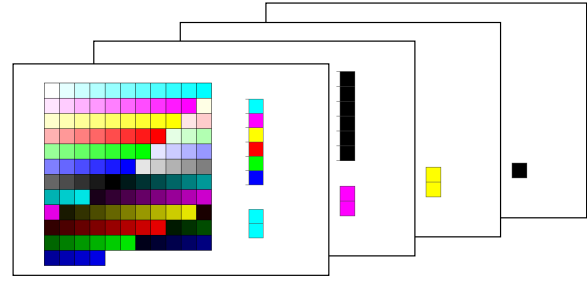
Figure 3. The set of images to obtain measured data for the training phase. The front image must be printed first, and includes the ramp of inks mixtures for model training. The column of patches on the right of training samples includes the patches for overprints measurements. The print of the second image on the same sheet of the first one produces the overprint of black on primary inks and secondary (R,G,B) colors. The print of the third and the last image produce the overprint of the three inks cyan, magenta and yellow, and the overprint of the four inks.
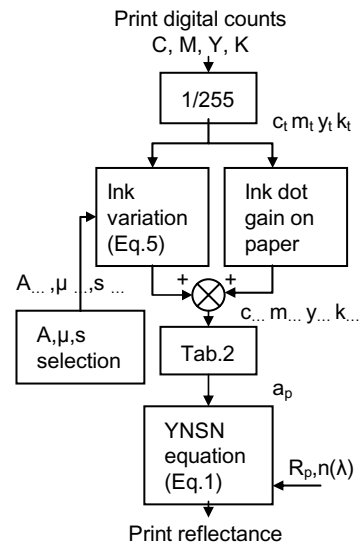
Figure 4. A graphical representation of the model.

Table 2. Error Statistics.

Data Set	ΔE^*_{ab} Avg.	ΔE^*_{ab} 95%	RMS% Avg.	RMS% Max.	RMS% S. dev.
Training	1.471	4.434	0.495	2.176	0.451
Test	1.541	3.956	0.585	2.397	0.461
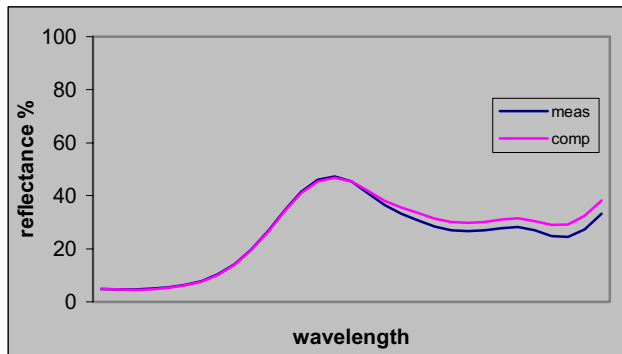
Figure 5. Plot of the worst test set result, according to RMS error.
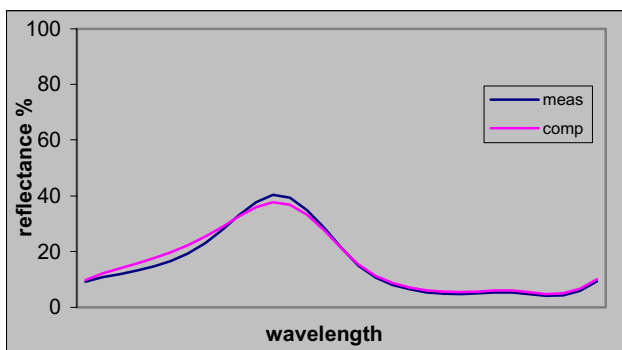
Figure 6. Plot of the worst test set result, according to the CIELAB ΔE^*_{ab} error. The colorimetric error between measured and computed spectrum is 8.858.

In literature, many strategies have been proposed to improve the accuracy of Neugebauer models, not always with the extent to better modeling inks dot gain and interactions. Approaches exist that assumes that the Neugebauer primaries can be optimized, or increased in number to face the problem with cellular methods, that treat the Neugebauer equation as an interpolation model.[2,10] This last strategy has been adopted in spectral-based characterization applications.[20] Despite a direct comparison of methods performance is not possible, due to the differences in devices and test sets with reported performance,[21] we however underline that our method is comparable in performance with cellular approaches. A similar conclusion holds for methods based on neural networks.[22] Respect with the mentioned techniques, however, it requires printing and measuring a smaller training set.

Conclusions

In this paper we have proposed a novel method to represent dot gain and interaction among inks in printer modeling throughout the Yule Nielsen Spectral Neugebauer model. The feasibility of our approach has been verified in the spectral-based characterization of an inkjet printer producing

a spectral accuracy in terms of mean root mean squared error of 0.59% and of 1.54 ΔE^*_{ab}.

References

1. B. Hill, Color capture, color management and the problem of metamerism: does multispectral imaging offer the solution?, Proc. IS&T/SPIE Dev.-Independent Color, Color Hardcopy and Graphics Arts V, (2000).
2. R. Balasubramanian, Optimization of the spectral Neugebauer model for printer characterization, Journal of Electronic Imaging, 8, 2, (1999).
3. K. Iino and R. S. Berns, A Spectral Based Model of Color Printing that Compensates for Optical Interactions of Multiple Inks, AIC Color 97, Proc. 8th Congress International Colour Association, (1997).
4. D. Tzeng, R. S. Berns, Spectral-Based Six-Color Separation Minimizing Metamerism, Proc. CIC, (2000).
5. S. Gustavson, The Color Gamut of Halftone Reproduction, Proc. CIC, (1996).
6. J. S. Arney, T. Wu, C. Blehm, Modeling the Yule-Nielsen Effect on Color Halftones, Proc. CIC, (1997).
7. J. S. Arney, T. Wu, C. Blehm, Modeling the Yule-Nielsen Effect on Color Halftones, Journal of Imaging Science and Technology, 42, 4, (1998).
8. P. Emmel, R. D. Hersch, A Unified Model for Color Prediction of Halftoned Print, Journal of Imaging Science and Technology, 44, 4, (2000).
9. P. Emmel, R. D. Hersch, Modeling Ink Spreading for Color Prediction, Journal of Imaging Science and Technology, 46, 3, (2002).
10. A. U. Agar, J. P. Allebach, An Iterative Cellular YNSN Method for Color Printer Characterization, Proc. CIC, (1998).
11. M. Xia, G. Sharma, A. M. Tekapl, End-to-End Color Printer Calibration by Total Least Square Regression, IEEE Trans. Image Processing, 8, 5, (1999).
12. C. Lana, M. Rotea, D. Viassolo, Characterization of Color Printers Using Robust Parameter Estimation, Proc. CIC, 2003.
13. G. L. Rogers, Neugebauer Revisited: Random Dots in Halftone Screening, Color Research and Application, 23, 2, (1998).
14. I. Amidror, R. D. Hersch, Neugebauer and Demichel: Dependence and Independence in n-Screen Superpositions for Colour Printing, Color Research and Applications, 25, 4, (2000).
15. R. Balasubramanian, A spectral Neugebauer model for dot-on-dot printers, Proc. SPIE vol. 2413, (1995).
16. E. J. Stollnitz, V. Ostromoukhov, D. H. Salesin, Reproducing Color Images Using Custom Inks, Proc. of SIGGRAPH'98, (1998).
17. D. Tzeng, Spectral-based color separation algorithm development for multiple-ink color reproduction, Ph.D. Thesis, R.I.T., Rochester, (1999).
18. J. A. Stephen Viggiano, Modeling the Color of Multi-Colored Halftones, Proc. TAGA, (1990).

19. D. R. Wyble, R. S. Berns, A Critical Review of Spectral Models Applied to Binary Color Printing, Color Research and Application, 25, 1, (2000).
20. Y. Chen, R. S. Berns, L. A. Taplin, F. H. Imai, A Multi-Ink Color-Separation Algorithm Maximizing Color Constancy, Proc. CIC, (2003).
21. R. Bala, Device Characterization, Chapter 5 of Digital Color Imaging Handbook, Edited by G. Sharma, CRC Press, (2003).
22. R. Schettini, D. Bianucci, G. Mauri, S. Zuffi, An Empirical Approach for Spectral Color Printers Characterization, Proc. CGIV, (2004).

Biography

Silvia Zuffi was born in Rimini, Italy, on July 3, 1969. She graduated in 1995 with the Laurea in Electronic Engineering at University of Bologna, Italy. From 1995 through 1997 she was a Computer Software Engineer, then she joined the Movement Analysis Laboratory at the Istituti Ortopedici Rizzoli, Bologna, Italy. Since 1999 she has been a Research Scientist in Italian National Research Council (CNR). Her current research interests include cross-media color reproduction, multispectral imaging and spectral-based printer characterization.